(Strange) Meson Interferometry at RHIC

Sven Soff*§, Steffen A. Bass†, David H. Hardtke*, and Sergey Y. Panitkin‡

* Nuclear Science Division 70-319, Lawrence Berkeley National Laboratory, One Cyclotron Road, Berkeley, CA94720, USA
† Department of Physics, Duke University, Durham, NC27708, USA, and RIKEN BNL Research Center, Brookhaven National Laboratory, Upton, NY11973, USA
‡ Physics Department, Brookhaven National Laboratory, PO Box 5000, Upton, NY11973, USA

Abstract. We make predictions for the kaon interferometry measurements in Au+Au collisions at the Relativistic Heavy Ion Collider (RHIC). A first order phase transition from a thermalized Quark-Gluon-Plasma (QGP) to a gas of hadrons is assumed for the transport calculations. The fraction of kaons that are directly emitted from the phase boundary is considerably enhanced at large transverse momenta $K_T \sim 1\,\mathrm{GeV/c}$. In this kinematic region, the sensitivity of the $R_{\mathrm{out}}/R_{\mathrm{side}}$ ratio to the QGP-properties is enlarged. The results of the 1-dimensional correlation analysis are presented. The extracted interferometry radii, depending on K_T, are not unusually large and are strongly affected by finite momentum resolution effects.

1. Introduction

We discuss predictions for the kaon interferometry measurements in Au+Au collisions at the Relativistic Heavy Ion Collider (RHIC) that accelerates the nuclei up to nucleon-nucleon center-of-mass energies of $\sqrt{s}_{NN} = 200\,\mathrm{GeV}$. Correlations of identical particle pairs, sometimes also called HBT interferometry, provide important information on the space-time extension of the particle emitting source as produced for example in ultrarelativistic heavy ion collisions [1]. In this case, QCD lattice calculations have predicted a transition from quark-gluon matter to hadronic matter at high temperatures. For a first-order phase transition, large hadronization times have been expected due to the associated large latent heat as compared to a purely hadronic scenario [2, 3, 4]. Entropy has to be conserved while the number of degrees of freedom is reduced throughout the phase transition. Thus, one has expected a considerable jump in the magnitude of the interferometry radius parameters and the emission duration once the energy density is large enough to produce quark-gluon matter. Two alternative scenarios of the space-time evolution, with and without a phase transition, are illustrated in Fig. 1 in the z-t-diagram. After the collision of the two nuclei, each with nucleon number A, the system is formed at some eigen-time τ (indicated by the hyperbola) and the initial expansion proceeds either in a hadronic state (left-hand side) or in a state dominated by partonic degrees of freedom, for example a quark-gluon plasma (QGP) (right-hand side). In the latter case, the formation of a mixed phase, leads to large hadronization times and thus to rather long emission durations. The

§ ssoff@lbl.gov

freeze-out is defined as the decoupling of the particles, i.e., the space-time coordinates of their last (strong) interactions. Summarizing this idea illustrated in Fig. 1, the interferometry of identical particle pairs and in particular the excitation function of the interferomtry parameters have been considered as an ideal tool to detect the existence and the properties of a transition from a thermalized quark-gluon plasma to hadrons. Quantities of great interest are for example the critical temperature T_c or the latent heat of the phase transition. The prolonged emission duration should lead in particular to an increase of the effective source size in the *outward* direction, i.e., parallel to the transverse pair velocity. One also expects correlation lengths depending on the specific entropy of the collision. For recent reviews see for example [5, 6].

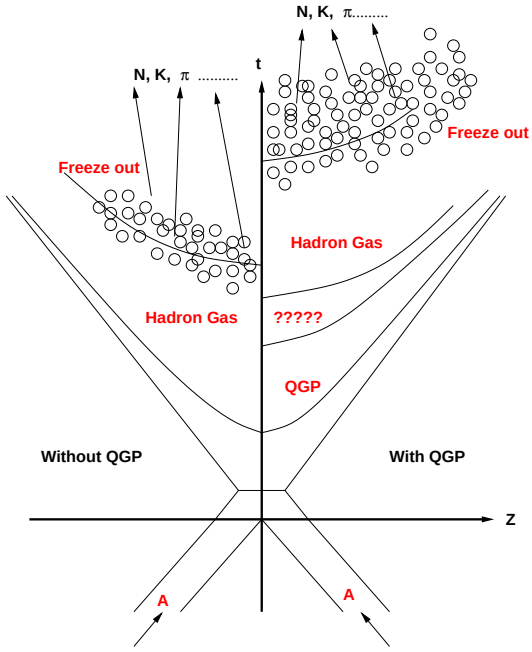

Figure 1: Illustration of the space-time evolution in the z-t-diagram with (right) and without (left) a phase transition. Proceeding through a first-order phase transition with a large latent heat should lead to large hadronization times, thus yielding eventually large interferometry radius parameters and emission duration.

2. Space-time evolution and kaon interferometry

Here, we discuss calculations based on a relativistic two-phase dynamical transport model that describes the early quark-gluon plasma phase by hydrodynamics and the later stages, after hadronization from the phase boundary of the mixed phase, by microscopic transport of the hadrons. For the initial dense (hydrodynamical) phase of a QGP a bag model equation of state exhibiting a first order phase transition is employed [4, 7]. Hence, a phase transition in local equilibrium that proceeds through the formation of a mixed phase, is considered. A crossover [4, 8] or a rapid out-of-equilibrium phase transition similar to spinodal decomposition [9] may yield smaller radii and emission times. In the hadronic phase, resonance (de)excitations and binary collisions are modeled based on cross sections and resonance properties as measured in vacuum [10, 11]. A detailed description of this relativistic hybrid transport model and its predictions can be found elsewhere [12, 13, 14]. The particular differences and advantages compared to *pure* hydrodynamical calculations are for example due to the explicit calculation of the freeze-out phase-space distributions. Moreover, the system evolution in the later dilute stages is based on cross sections

and resonance (de)excitations are possible. The assumption of *ideal* hydrodynamics might be not valid anymore in these later stages close to a freeze-out criterion like a fixed temperature $T_{\rm fr}$. Another important example will be shown below (Fig. 5), demonstrating the possibility of direct emission from the early phase in this transport model used here. The mean freeze-out times are strongly depending on the transverse momentum of the particles as illustrated in Fig. 2 for kaons and anti-kaons. Obviously, large transverse momentum kaons are correlated to early mean freeze-out times. The difference between kaons and anti-kaons is almost negligible, only at very small p_t anti-kaons may be emitted a tiny instant later due a small finite net-baryon number in the system. (The K^-N cross section is considerably larger than the K^+N cross section.) Otherwise the $K\pi$ cross section, dominated by the K^*, yields almost identical freeze-out distributions for kaons and anti-kaons. Strangeness distillation [15] due to local large net-baryon numbers leading to emission asymetries that are observable in K^+K^- correlations [16] is not considered here.

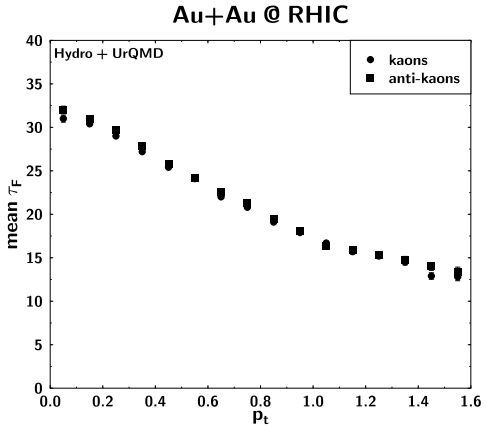

Figure 2: Mean freeze-out time τ_F as a function of transverse momentum p_t for kaons and anti-kaons in Au+Au collisions at RHIC. High p_t kaons are correlated with early freeze-out times.

The coordinate system for the correlation analysis is defined by the *long* axis (z) (parallel to the beam axis), the *out* direction (parallel to the transverse momentum vector $\mathbf{K_T} = (\mathbf{p_{T1}} + \mathbf{p_{T2}})/2$ of the pair), and the *side* direction (perpendicular to both). Due to the definition of the *out* and *side* direction, $R_{\rm out}$ probes the spatial *and* temporal extension of the source while $R_{\rm side}$ only probes the spatial extension. It has been suggested that the ratio $R_{\rm out}/R_{\rm side}$ should increase strongly once the initial entropy density s_i becomes substantially larger than that of the hadronic gas at T_c [4]. The Gaussian radius parameters can be obtained from a saddle-point integration over the classical phase space distribution of the hadrons at freeze-out (points of their last (strong) interaction) that is identified with the Wigner density of the source, $S(x, K)$ [17, 6, 18, 19].

$$R^2_{\rm side}(\mathbf{K_T}) = \langle \tilde{y}^2 \rangle(\mathbf{K_T}) \,, \tag{1}$$

$$R^2_{\rm out}(\mathbf{K_T}) = \langle (\tilde{x} - \beta_t \tilde{t})^2 \rangle(\mathbf{K_T}) = \langle \tilde{x}^2 + \beta_t^2 \tilde{t}^{\,2} - 2\beta_t \tilde{x}\tilde{t} \rangle(\mathbf{K_T}) \,, \tag{2}$$

$$R^2_{\rm long}(\mathbf{K_T}) = \langle (\tilde{z} - \beta_l \tilde{t})^2 \rangle(\mathbf{K_T}) \,, \tag{3}$$

with

$$\tilde{x}^\mu(\mathbf{K_T}) = x^\mu - \langle x^\mu \rangle(\mathbf{K_T}) \tag{4}$$

being the space-time coordinates relative to the momentum dependent *effective source*

centers. The average in (1)-(3) is taken over the emission function, i.e.,

$$\langle f \rangle(K) = \frac{\int d^4x f(x) S(x,K)}{\int d^4x S(x,K)} \tag{5}$$

with $K = (E_K, \mathbf{K})$. In the *osl* system $\beta = (\beta_t, 0, \beta_l)$, where $\beta = \mathbf{K}/E_K$ and $E_K = \sqrt{m^2 + \mathbf{K}^2}$ (on-shell approximation). For small $\tilde{x}$-$\tilde{t}$ correlations, i.e. in particular at small K_T, $R_{\rm out}$ is increased relative to $R_{\rm side}$ if the duration of emission $\Delta\tau = \sqrt{\langle \tilde{t}^{\,2} \rangle}$ is large [2, 3, 4]. Strong (positive) $\tilde{x}$-$\tilde{t}$-correlations or large spatial anisotropies in *out*- and *side*-direction ($\langle \tilde{y}^2 \rangle > \langle \tilde{x}^2 \rangle$) may, in principle, lead to $R_{\rm out} \leq R_{\rm side}$. This is not seen within the model scenario discussed here.

From eqs. (1) and (2) one can easily calculate the ratio $R_{\rm out}/R_{\rm side}$ for kaons. Kaons, compared to pions, are expected to be less contaminated by resonance decays [18, 20]. In addition the kaon phase space density is much smaller than the pion density [21]. As a consequence, higher multiparticle correlation effects (that may be important for pions at RHIC energies [22]) are possibly under much better control for kaons. Fig. 3 shows the kaon $R_{\rm out}/R_{\rm side}$ ratio for SPS (initial conditions $\tau_i = 1\,$fm/c (thermalization eigen-time) and $s/\rho_B = 45$ (specific entropy density)) and RHIC ($\tau_i = 0.6$, $s/\rho_B = 200$) [14]. The bag parameter B is varied from 380 MeV/fm^3 to 720 MeV/fm^3. This corresponds to a variation of the critical temperature from $T_c \approx 160\,$MeV to $T_c \approx 200\,$MeV.

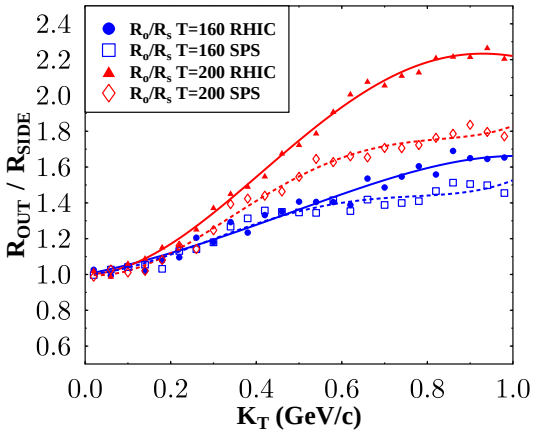

Figure 3: $R_{\rm out}/R_{\rm side}$ as obtained from eqs. (1) and (2) for kaons at RHIC (Au+Au, $\sqrt{s_{NN}} = 200\,$GeV) (full symbols) and at SPS (Pb+Pb, $\sqrt{s_{NN}} = 17.4\,$GeV) (open symbols), as a function of K_T for critical temperatures $T_c \simeq 160\,$MeV and $T_c \simeq 200\,$MeV, respectively.

For small K_T, the ratio $R_{\rm out}/R_{\rm side}$ increases slowly compared to the faster rise for pions [23]. This is due to the different masses yielding different flow velocities at the same K_T (see eq. (2)). Apparently, the sensitivity to the critical temperature T_c and the specific entropy density increases strongly with K_T. For higher T_c the hadronization is faster but the subsequent hadronic rescattering phase lasts longer. It was shown that this dissipative hadronic phase dominates the radii for pions [23]. The ratio $R_{\rm out}/R_{\rm side}$ is always larger than unity and reaches values on the order of $\approx 1.5-2$ at large K_T. This value is considerably smaller than former expectations (e.g. [4, 24]). On the other hand, first RHIC data for pion correlations show ratios that do not increase with K_T and are even smaller than unity [25, 26]. This completely new behaviour has not been seen at SPS energies (see e.g. [27]). However, new data by the CERES collaboration show a similar trend [28]. This observation would hint at a rather explosive scenario with very short emission times, not compatible with a picture of a thermalized quark-gluon plasma hadronizing via a first-order phase transition to an interacting hadron gas [23]. Rather a shell-like emission as illustrated in Fig. 4

would be prefered. Thus, the further study of two-particle interferometry will provide extremly important information e.g. on the hadronization process or the question of thermalization in ultrarelativistic heavy ion collisions. Also, the comparison of pion and kaon interferometry data may further clarify the situation.

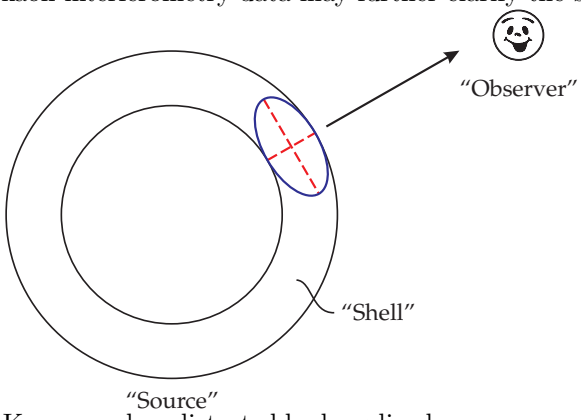

Figure 4: Illustration of a shell-like emission. The surface emission geometry corresponds to small values of the ratio $R_{\rm out}/R_{\rm side}$, indicated by the two dashed lines in the emission volume element relevant for an observer. The dashed line in the direction to the observer corresponds to the *out* direction, the orthogonal line is the *side* direction.

Kaons are less distorted by long-lived resonances and escape the opaque hadronic phase easier (compared to pions). About 30% of the kaons at $K_T \sim 1\,\mathrm{GeV/c}$ are directly emitted from the phase-boundary (for $T_c \approx 160\,\mathrm{MeV}$) as can be seen in Fig. 5. Complementary, we have seen already that large K_T kaons and their $R_{\rm out}/R_{\rm side}$ ratio exhibit a strong sensitivity on the QCD equation of state. The fraction of resonance decays (K*'s,...) is still quite large and decreases with K_T from about 70% to 50%. For the higher T_c ($\simeq 200\,\mathrm{MeV}$), hadronization is earlier and the hadronic phase lasts longer, such that the system is more opaque for direct emission than in the lower T_c case.

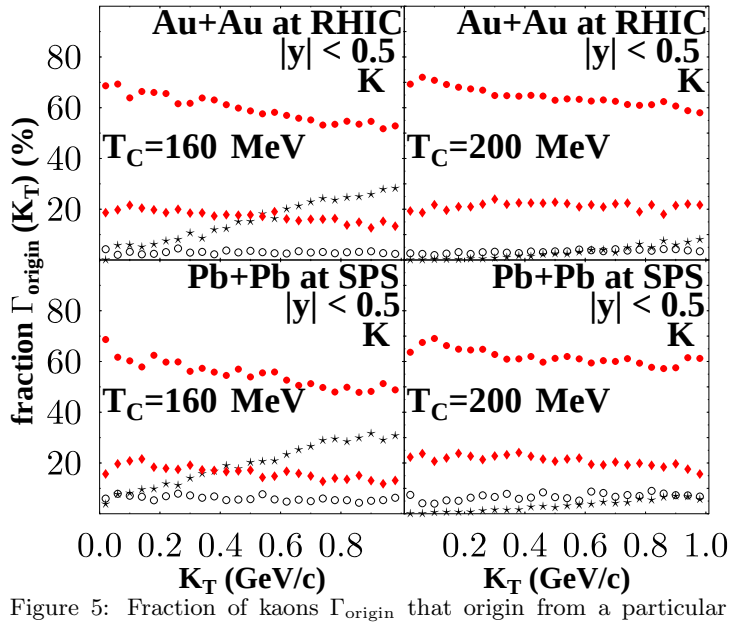

Figure 5: Fraction of kaons $\Gamma_{\rm origin}$ that origin from a particular reaction channel prior to freeze-out. These are resonance decays (full circles), direct emission from the phase boundary (stars), elastic meson-meson (diamonds), or elastic meson-baryon (open circles) collisions. The upper and lower diagrams are for RHIC and SPS initial conditions for $T_c \simeq 160\,\mathrm{MeV}$ (left) and $T_c \simeq 200\,\mathrm{MeV}$ (right), respectively.

We now calculate the one-dimensional kaon kaon correlation functions $C_2(Q_{\rm inv})$ for various K_T-bins and determine the corresponding fit parameters. The corresponding results for the three-dimensional analysis in the *out-side-long* coordinate system are presented in [14]. The parameters $R_{\rm inv}$ and λ_1 of the correlation functions are obtained by fitting a Gaussian as

$$C_2(Q_{\rm inv}) = 1 + \lambda_1 \exp(-Q_{\rm inv}^2 R_{\rm inv}^2)\,. \tag{6}$$

The correlation functions themselves are calculated from the phase space distributions of kaons at freeze-out using the *correlation after burner* by Pratt [2, 19]. The correlation functions can be calculated as

$$C_2(\mathbf{p_1},\mathbf{p_2}) \simeq 1 + \frac{\int \mathrm{d}^4x S(x,\mathbf{K}) \int \mathrm{d}^4y S(y,\mathbf{K}) \exp\left(2ik\cdot(x-y)\right)}{|\int \mathrm{d}^4x S(x,\mathbf{K})|^2}\,. \tag{7}$$

with $2\mathbf{K} = \mathbf{p_1} + \mathbf{p_2}$, $2\mathbf{k} = \mathbf{p_1} - \mathbf{p_2}$, and $2k^0 = E_{p_1} - E_{p_2}$.

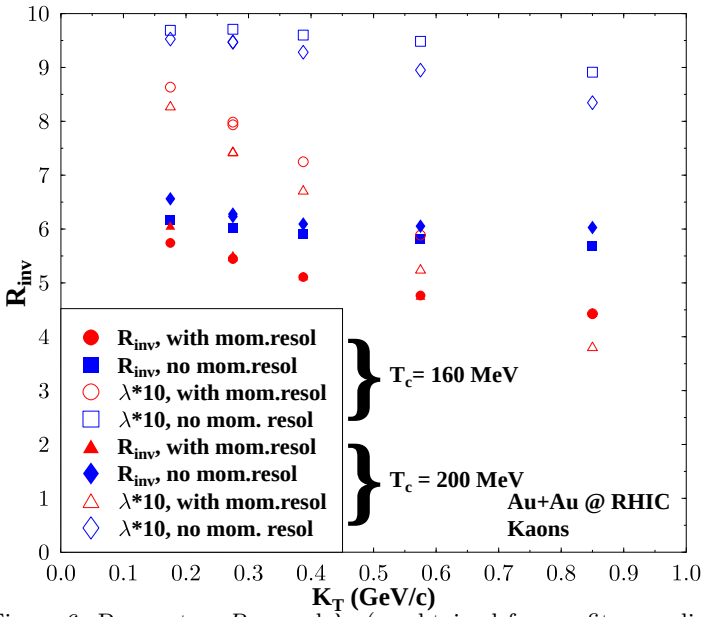

Figure 6: Parameters $R_{\rm inv}$ and λ_1 (as obtained from a fit according to eq. (6)) as a function of K_T for kaons in Au+Au collisions at RHIC for critical temperatures $T_c \simeq 160\,\mathrm{MeV}$ (circles, squares) and $T_c \simeq 200\,\mathrm{MeV}$ (triangles, diamonds), respectively. Calculations with and without taking momentum resolution effects into account are shown.

The results for RHIC are shown in Fig. 6. The λ_1 intercept parameters are multiplied by a factor 10. The correlation functions have been calculated for $T_c \approx 160\,\mathrm{MeV}$ (circles and squares) and $T_c \approx 200\,\mathrm{MeV}$ (triangles and diamonds). Moreover, calculations with and without taking finite momentum resolution (*f.m.r.)* effects have been performed. In the first case, the *true* particle momentum p obtains an additional random component. This random component is assumed to be Gaussian with a width δp. A *f.m.r.* of $\approx 2\%$ of the center of each K_T bin is considered, a value assumed for the STAR detector [25]. The relative momenta of pairs are then calculated from these modified momenta. However, the correlator is calculated with the *true* relative momentum. $R_{\rm inv}$ is on the order of $5.5-6.5\,\mathrm{fm}$ without and $4.5-6\,\mathrm{fm}$ with taking *f.m.r.* into account. Hence, $R_{\rm inv}$ is reduced by the *f.m.r.*. This reduction

grows with K_T. For the one-dimensional fit parameters, there is hardly a sensitivity to the critical temperature. However, the known trend (larger radii for higher T_c due to a prolonged hadronic phase) is also indicated in these results. The sensitivity to the specific entropy density, another initial condition, is known to be rather weak [23], even for a change from SPS to RHIC initial conditions, due to the dominance of the late soft hadronic interactions. Hence, the differences in the correlation parameters between, for example, the RHIC 130 GeV and 200 GeV energies are minute; (the number of charged particles at midrapidity increases only by about 15%). Preliminary analysis of STAR KK data (not yet corrected for *f.m.r.*) at $\sqrt{s}_{NN} = 130\,\mathrm{GeV}$ gives a value of $R_{\mathrm{inv}} = 4.5 \pm 0.3\,\mathrm{fm}$ (at $150\,\mathrm{MeV} < K_T < 400\,\mathrm{MeV}$ and rather central (11%) collisions) ($\lambda_1 = 0.92 \pm 0.13$) [29], which is almost compatible to the calculations that take *f.m.r.* into account. The λ_1 intercept parameters are almost constant without *f.m.r.* effects but strongly decrease when taking them into account. For illustration, let us consider particle pairs with a small *true* relative momentum q that will be redistributed by the random momentum smearing to, on the average, larger relative momenta $\tilde{q}$. Thus, the area around $q \approx 0$ is depleted from these *true* low momentum pairs that carry the full correlation strength. Complementary, some pairs with a larger *true* q (and thus with a weaker correlation strength) are redistributed to the small $\tilde{q}$ area. As a consequence, the *correlation strength is transported to larger q values*. Thus, the correlation function gets broader and the radius parameters become smaller. The strong decrease of λ_1 with K_T is due to the absolute larger momentum smearing at high K_T. *True* correlated pairs at low q are transported more likely to larger $\tilde{q}$ values. This reduced correlation strength in the first q bins causes the small λ_1 values at larger K_T. Recent experimental data (corrected for *f.m.r.*!) for central Pb+Pb collisions at $\sqrt{s} = 17.4\,\mathrm{GeV}$ yield $R_{\mathrm{inv}} = 6.2 \pm 0.4 \pm 0.9\,\mathrm{fm}$ at low transverse momenta ($\langle p_t \rangle = 250\,\mathrm{MeV}$) and $R_{\mathrm{inv}} = 3.3 \pm 0.6\,\mathrm{fm}$ at high transverse momenta ($\langle p_t \rangle = 910\,\mathrm{MeV}$) [30]. The corresponding λ_1 parameters are reported as $\lambda_1 = 0.84 \pm 0.11 \pm 0.19$ and $\lambda_1 = 0.47 \pm 0.12$ for the low and high p_t set, respectively.

3. Summary

The calculation of kaon correlation parameters for Au+Au collisions at RHIC energies, assuming a first-order phase transition from a thermalized QGP to a gas of hadrons shows

- an increasing $R_{\mathrm{out}}/R_{\mathrm{side}}$ ratio with K_T (larger than unity),
- an increasing sensitivity of the $R_{\mathrm{out}}/R_{\mathrm{side}}$ ratio with K_T,
- a strong (30%) direct emission component from the phase boundary at large $K_T \sim 1\,\mathrm{GeV/c}$,
- no unusually large radius parameters R_{inv} that are reduced due to finite momentum resolution effects,
- λ_1 intercept parameters that get strongly reduced due to finite momentum resolution,
- the reduction of R_{inv} and λ_1 grows with K_T.

The kaon interferometry measurements at RHIC (at high K_T) will be, in combination with the pion data, an utmost important and valuable probe of the space-time dynamics (close to the phase boundary) and to the properties of the phase transition.

Acknowledgments

This work is supported by the Alexander von Humboldt-Foundation through a Feodor Lynen Fellowship (SS) and the Gesellschaft für Schwerionenforschung (Darmstadt). We thank A. Dumitru for many helpful comments, the UrQMD collaboration for permission to use the UrQMD transport model and S. Pratt for providing the correlation program CRAB. SS acknowledges support from DOE Grant No. DE-AC03-76SF00098 and SAB from DOE Grant No. DE-FG02-96ER40945 and DE-AC02-98CH10886.

References

[1] Kopylov G I, Podgoretsky M I 1972 *Sov. J. Nucl. Phys.* **15** 219; Shuryak E 1973 *Phys. Lett.* B **44** 387; Gyulassy M, Kauffmann S K, Wilson L W 1979 *Phys. Rev.* C **20** 2267; Makhlin A, Sinyukov Y 1988 *Z. Phys.* C **39** 69; Hama Y, Padula S 1988 *Phys. Rev.* D **37** 3237; Podgoretsky M I 1989 *Sov. J. Part. Nucl.* **20** 266

[2] Pratt S 1986 *Phys. Rev.* D **33** 1314; Bertsch G, Gong M, Tohyama M 1988 *Phys. Rev.* C **37** 1896

[3] Schlei B R, Ornik U, Plümer M, Weiner R M 1992 *Phys. Lett.* B **293** 275; Bolz J, Ornik U, Plümer M, Schlei B R, Weiner R M 1993 *Phys. Rev.* D **47** 3860

[4] Rischke D, Gyulassy M 1996 *Nucl. Phys.* A **608** 479

[5] Weiner R M 2000 *Phys. Rept.* **327** 249; Csörgő T 2000 *Preprint* hep-ph/0001233; Baym G 1998 *Acta Phys. Polon.* B **29** 1839

[6] Wiedemann U, Heinz U 1999 *Phys. Rept.* **319**, 145

[7] Von Gersdorff H, McLerran L, Kataja M, Ruuskanen P V 1986 *Phys. Rev.* D **34** 2755

[8] Zschiesche D, Schramm S, Stöcker H, Greiner W 2001 *Preprint* nucl-th/0107037

[9] Csörgő T, Csernai L 1994 *Phys. Lett.* B **333** 494; Heiselberg H, Jackson A D 1998 *Preprint* nucl-th/9809013; Rafelski J, Letessier J 2000 *Phys. Rev. Lett.* **85** 4695; Dumitru A, Pisarski R 2001 *Phys. Lett.* B **504** 282; Scavenius O *et al.* 2001 *Phys. Rev.* D **63** 116003; 2001 *Phys. Rev. Lett.* **87** 182302; Mishustin I 2001 *Nucl. Phys.* A **681** 56

[10] Bass S A *et al.* 1998 *Prog. Part. Nucl. Phys.* **41** 255; Bleicher M *et al.* 1999 *J. Phys. G: Nucl. Phys.* **25** 1859

[11] Soff S 2000 *Dissertation* (Univ. Frankfurt: Ibidem-Verlag) ISBN 3-89821-074-X

[12] Dumitru A and Rischke D 1999 *Phys. Rev.* C **59** 354

[13] Bass S A, Dumitru A 2000 *Phys. Rev.* C **61** 064909

[14] Soff S, Bass S A, Hardtke D, Panitkin S 2002 *Phys. Rev. Lett.* **88** 072301

[15] Greiner C, Koch P, Stöcker H 1987 *Phys. Rev. Lett.* **58** 1825; 1991 *Phys. Rev.* D **44** 3517; Spieles C *et al.* 1996 *Phys. Rev. Lett.* **76** 1776

[16] Soff S *et al.* 1997 *J. Phys.* G **23** 2095; *Phys. Lett.* B **446** 191

[17] Podgoretsky M I 1983 *Sov. J. Nucl. Phys.* **37** 272

[18] Gyulassy M, Padula S 1990 *Phys. Rev.* C **41** 21; 1989 *Phys. Lett.* B **217** 181

[19] Pratt S, Csörgő T, Zimanyi J 1990 *Phys. Rev.* C **42** 2646; Pratt S 1984 *Phys. Rev. Lett.* **53** 1219; 1994 *Phys. Rev.* C **49** 2722; Zajc W A 1987 *Phys. Rev.* D **35** 3396; Pratt S *et al.* 1994 *Nucl. Phys.* A**566** 103c

[20] Sullivan J P *et al.* 1993 *Phys. Rev. Lett.* **70** 3000

[21] Murray M 2002 contribution to this volume, *J. Phys. G: Nucl. Part. Phys.*

[22] Lednicky R, Lyuboshitz V, Mikhailov K, Sinyukov Y, Stavinsky A and Erazmus B 2000 *Phys. Rev.* C **61** 034901

[23] Soff S, Bass S A, Dumitru A 2001 *Phys. Rev. Lett.* **86** 3981

[24] Bernard S, Rischke D, Maruhn J, Greiner W 1997 *Nucl. Phys.* A **625** 473

[25] STAR Collaboration, Adler C *et al.* 2001 *Phys. Rev. Lett.* **87** 082301

[26] PHENIX Collaboration, Johnson S C *et al.* 2002 *Nucl. Phys.* A **698** 603

[27] Blume C for the NA49 collaboration 2001 talk given at Quark Matter 2001, Jan. 15–20, Stony Brook, NY, USA

[28] Appelshäuser H for the CERES collaboration 2002 talk given at the XXX International Workshop on Gross Properties of Nuclei and Nuclear Excitations, Jan. 13-19, Hirschegg, Austria

[29] Panitkin S for the STAR collaboration 2002 contribution to this volume, *J. Phys. G.: Nucl. Part. Phys.*

[30] NA44 Collaboration, Bearden I G *et al.* 2001 *Phys. Rev. Lett.* **87** 112301; 1999 *Nucl. Phys.* A **661** 435c